Supporting Information

Construction of Solvent-dependent Self-assembly Porous Ni(II) Coordinated Frameworks Effectively Catalysis for Chemical Transformation of CO_2

Zhen Zhou,[a] Lu Yang,[a] Yefei Wang,[a] Cheng He,*[a] Tao Liu[a] and Chunying Duan[ab]

[a]*State Key Laboratory of Fine Chemicals, Dalian University of Technology, Dalian 116024, China;* [b]*Collaborative Innovation Center of Chemical Science and Engineering, Tianjin, 300071, China.*

Contents

1. Crystallography data.

Table S1. Crystal data and structure refinements

Compounds	**Ni-**1	**Ni-**2
Empirical formula	$C_{15}H_8Ni_{0.75}O_{6.75}$	$C_{3.75}H_{2.25}Ni_{0.25}O_{1.34}$
Formula weight	340.25	83.45
T/K	220(2)	220(2)
Crystal system	Orthorhombic	Trigonal
Space group	*Pmna*	*P*6*/mmm*
a/Å	27.2662(6)	26.2500(4)
b/Å	11.5396(3)	26.2500(4)
c/Å	13.9678(3)	11.2436(5)
α/°	90	90
β/°	90	90
γ/°	90	120
V/Å^3	4394.84(18)	6709.6(3)
Z	8	24
D_{calc}/Mg m^{-3}	1.028	0.496
μ/mm^{-1}	0.696	0.440
F(000)	1384	1020
R_{int}	0.0317	0.0717
Data/parameters	3973 / 257	2312 / 80
GOF	1.147	1.047
R [$I > 2\sigma(I)$]^a	R_1 = 0.0921 wR_2 = 0.2896	R_1 = 0.0983 wR_2 = 0.3269
R indices (all data)^b	R_1 = 0.1003 wR_2 = 0.2963	R_1 = 0.1140 wR_2 = 0.3359
$\Delta\rho_{max,min}$/eÅ^{-3}	1.319 / -0. 836	1.041 / -0.578
CCDC number	1502000	1502001

$^aR_1 = \Sigma||F_o| - |F_c||/\Sigma|F_o|$; $^bwR_2 = \Sigma[w(F_o^2 - F_c^2)^2]/\Sigma[w(F_o^2)^2]^{1/2}$

2. Supplementary Structural Figures

Figure S1. The ball-stick mode of the 3D structural framework (a) and the topological net (b) of **Ni-1** along the *b* axis. All guest molecules and hydrogen atoms were omitted for clarity.

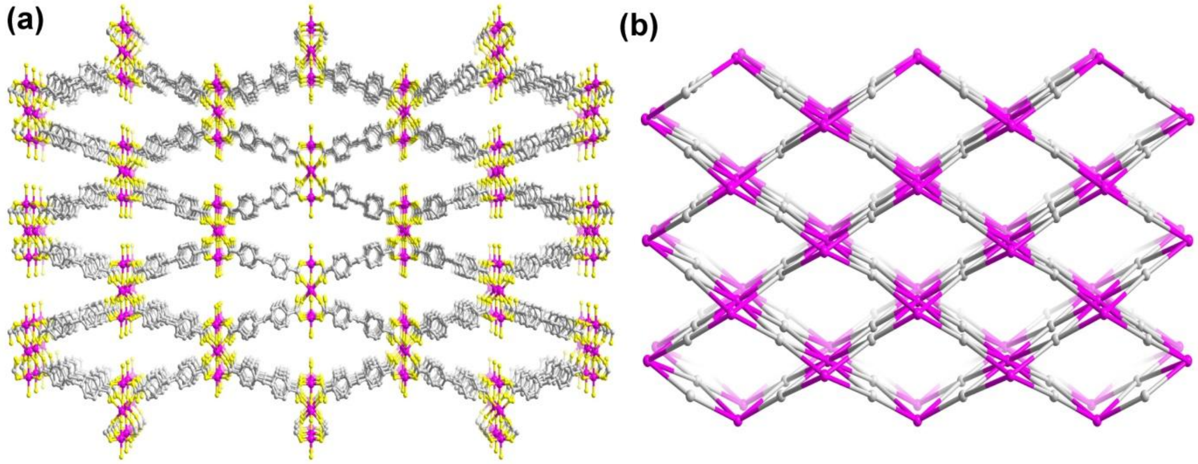

Figure S2. The ball-stick mode of the 3D structural framework (a) and the topological net (b) of **Ni-1** along the *c* axis. All guest molecules and hydrogen atoms were omitted for clarity.

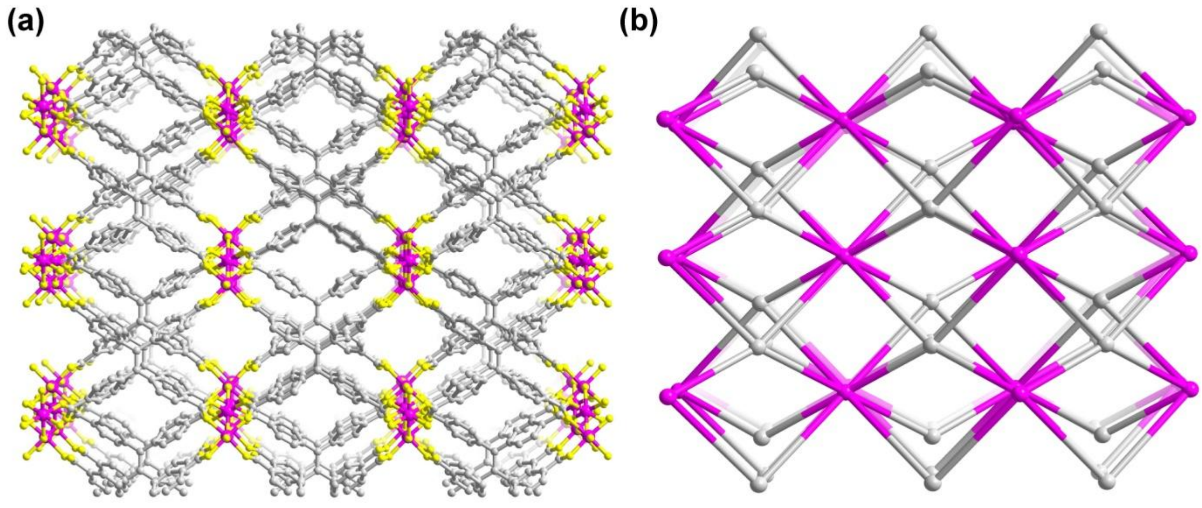

Figure S3. The ball-stick mode of the 3D structural framework (a) and the topological net (b) of **Ni-2** along the *c* axis. All guest molecules and hydrogen atoms were omitted for clarity.

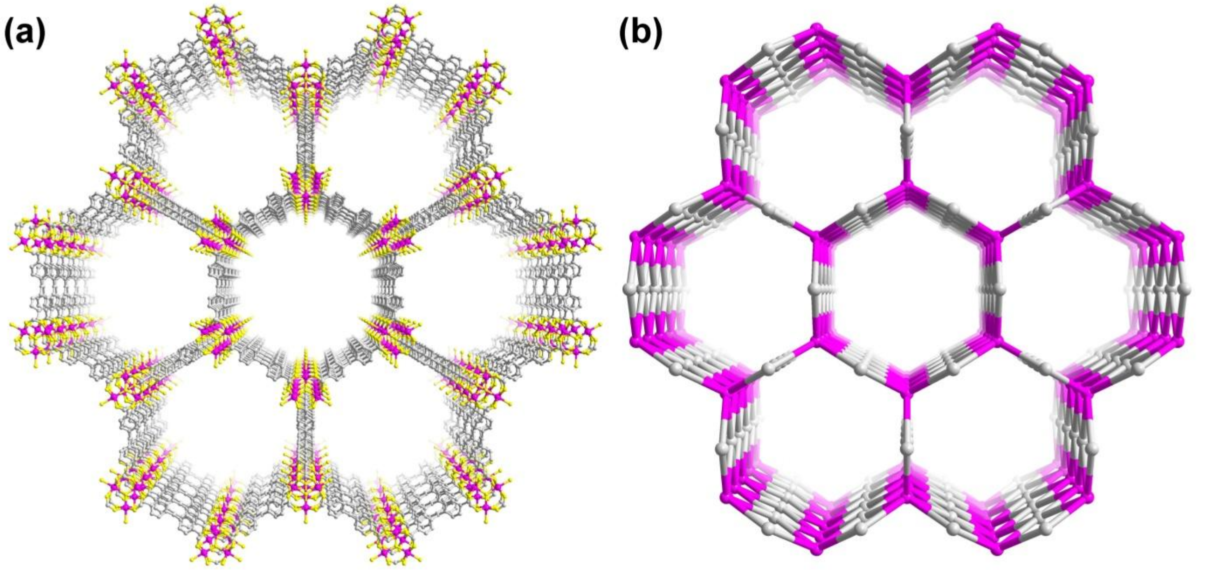

Figure S4. The ball-stick mode of the 3D structural framework (a) and the topological net (b) of **Ni-2** along the *b* axis. All guest molecules and hydrogen atoms were omitted for clarity.

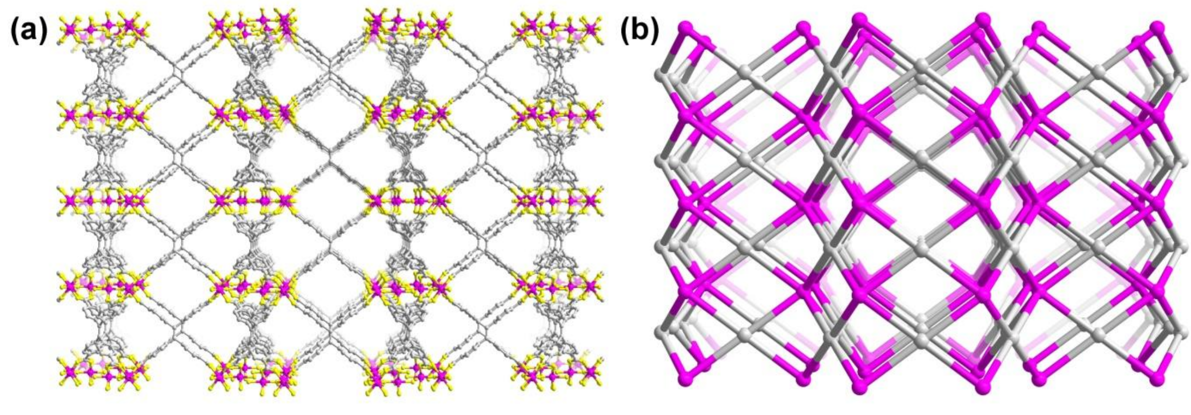

3. Characterizations of Catalysts

Figure S5. TG curve of as-synthesized **Ni-1** (black) and activated **Ni-1** (red).

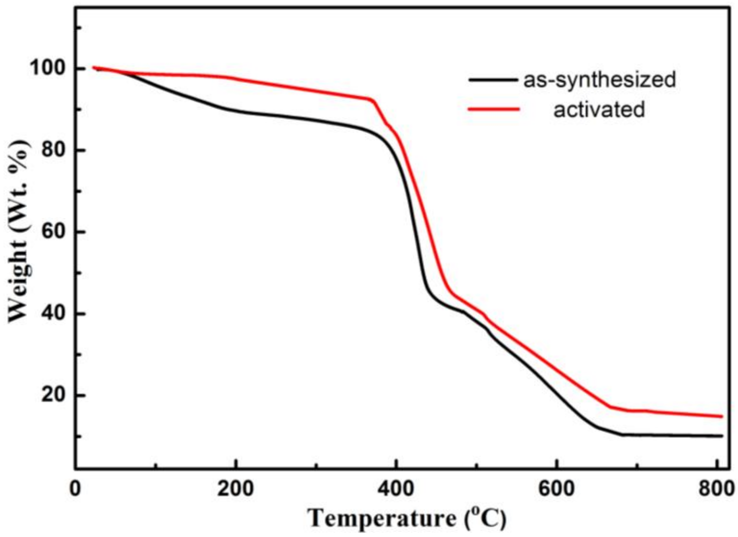

Figure S6. TG curve of as-synthesized **Ni-2** (black) and activated **Ni-2** (red)..

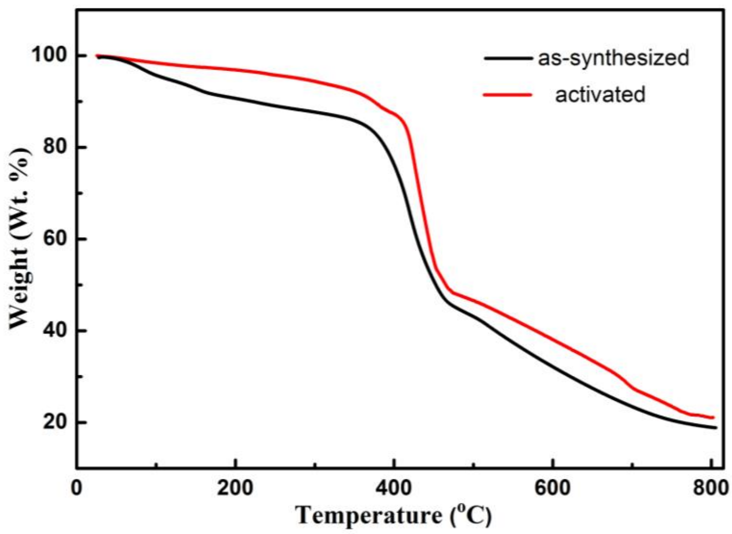

Figure S7. IR spectra of **Ni-1** and the samples after being dispersed in different solvents.

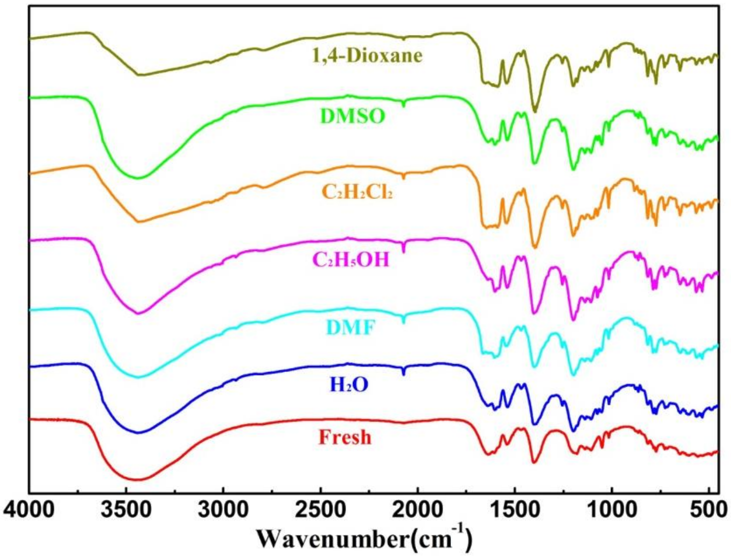

Figure S8. IR comparison between **Ni-2** and the samples after being dispersed in different solvents.

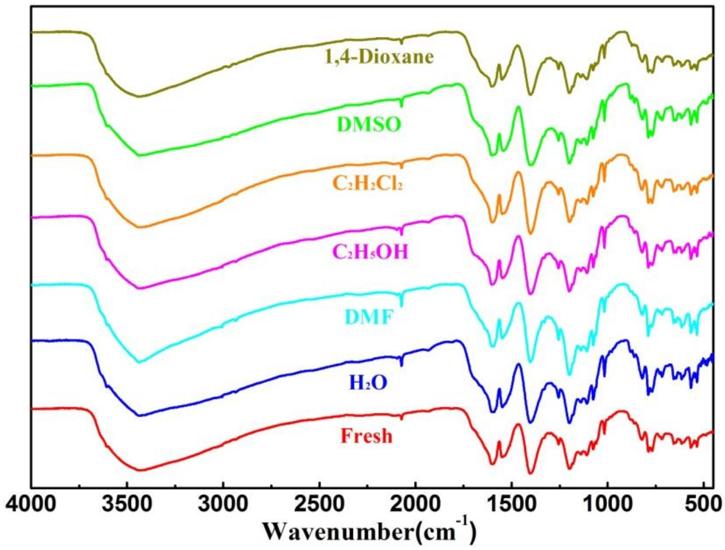

Figure S9. PXRD patterns of **Ni-1** (blue), its simulated pattern based on the single-crystal data (red) and the recycled catalyst after reactions (green).

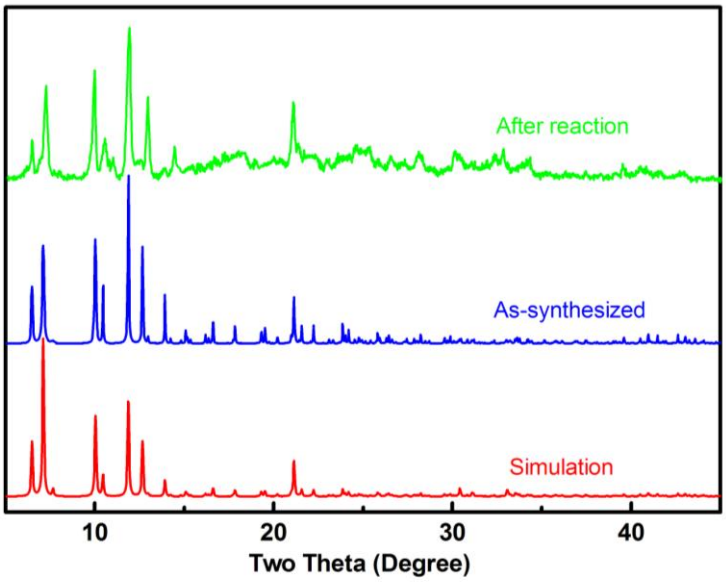

Figure S10. PXRD patterns of **Ni-2** (blue), its simulated pattern based on the single-crystal data (red) and the recycled catalyst after reactions (green).

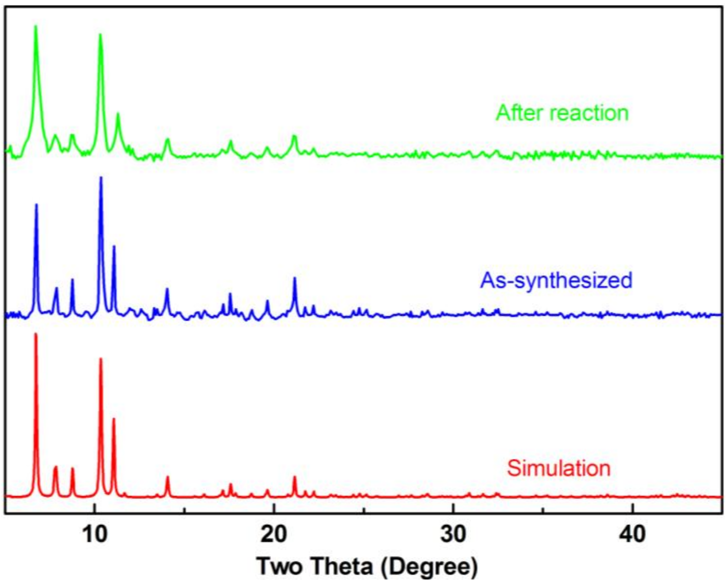

4. Catalysis Details

Table S2. Recyclability characterization of **Ni-1** and **Ni-2** in five runs for CO_2 cycloaddition with propylene oxide to produce propylene carbonate under the optimal conditions.

Entry	Yield (%)	
	Ni-1	Ni-**2**
Round 1	98	99
Round 2	97	99
Round 3	95	96
Round 4	95	93
Round 5	91	92

Table S3. Molecular Size of epoxides.[a]

Entry	Substrate	3D view	x (Å)	y (Å)	z (Å)
1			4.2	2.6	1.8
2	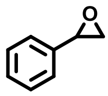	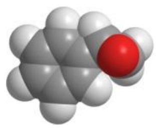	6.6	4.3	2.3
3	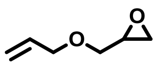	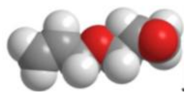	8.7	3.0	2.3
4	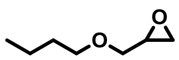	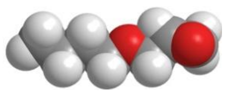	9.9	2.5	3.0
5	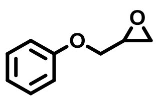	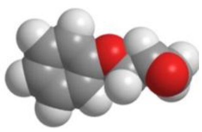	9.4	4.3	2.3
6	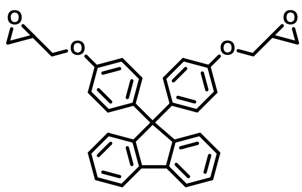	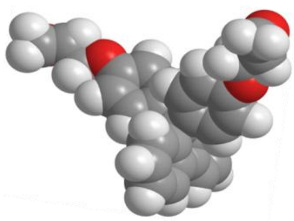	15.4	9.4	9.0

[a] The assumed structures and the molecular size were calculated by using the program Chem3D

Scheme S1. Proposed reaction mechanism for cycloaddition reactions from CO_2 and epoxides catalyzed by Ni-based MOF materials.

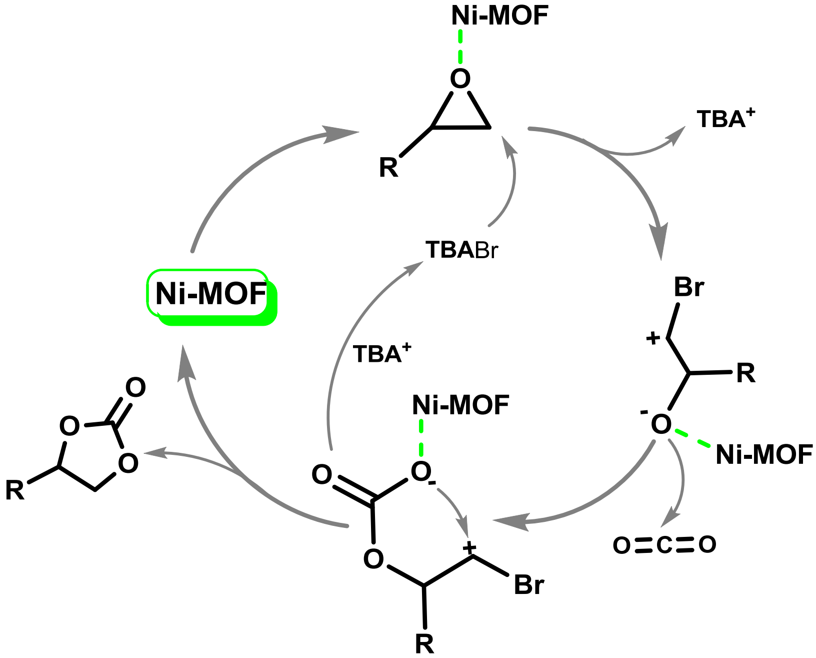

Figure S11. ^{1}H NMR spectra of 2a (400 MHz, $CDCl_3$): δ = 4.99–4.86 (1H, m), 4.63 (1H, t, *J* 8.1), 4.06 (1H, t, *J* 7.8), 1.51 (3H, d, *J* 6.2). Isolated yield: 94.6% (**Ni-1**), 96.5% (**Ni-2**).

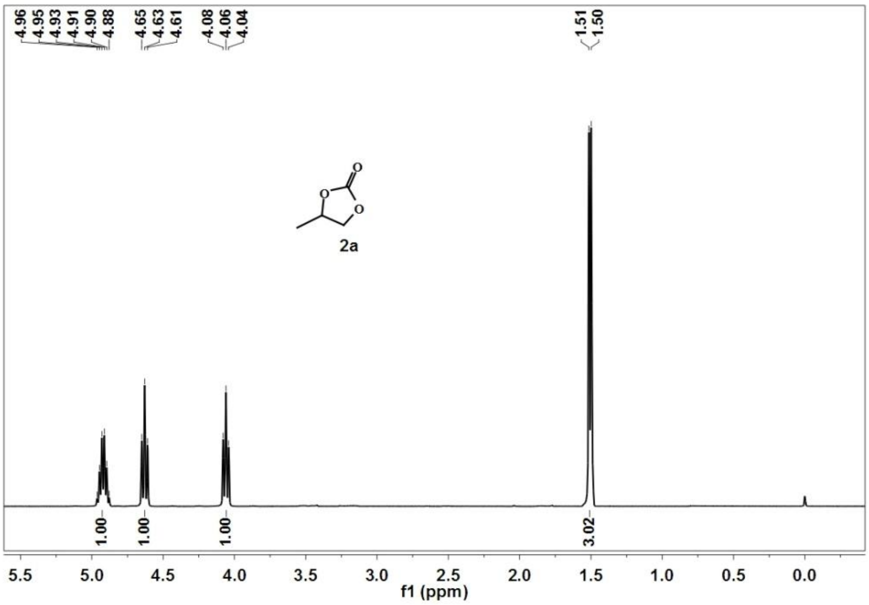

Figure S12. ^{1}H NMR spectra of 2b (400 MHz, $CDCl_3$): δ = 7.46–7.36 (3H, m), 7.34 (2H, dd, *J* 7.4, 2.1), 5.66 (1H, t, *J* 8.0), 4.78 (1H, t, *J* 8.4), 4.32 (1H, dd, *J* 8.6, 7.9). Isolated yield: 65.3% (**Ni-1**), 67.7% (**Ni-2**).

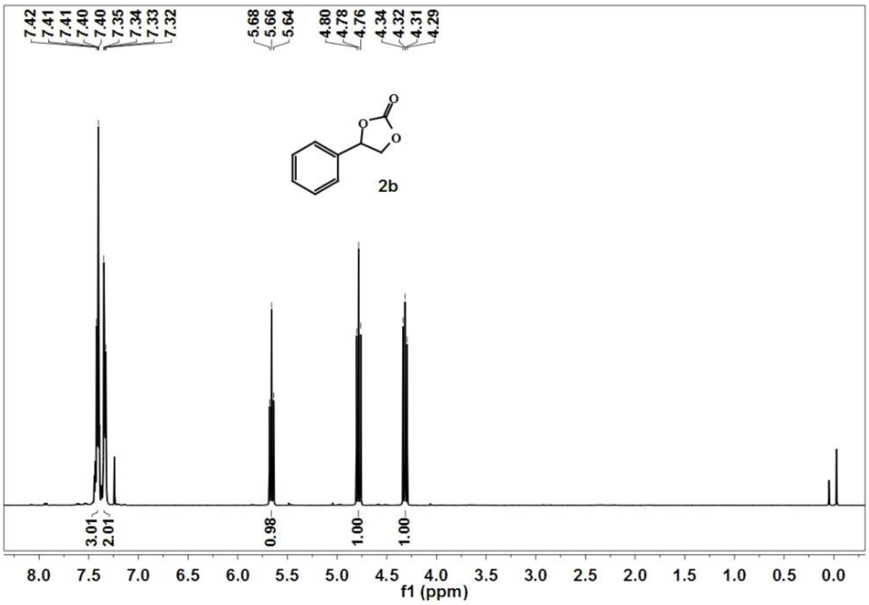

Figure S13. [1]H NMR spectra of 2c (400 MHz, $CDCl_3$): δ = 5.94–5.75 (1H, m), 4.86–4.72 (1H, m), 4.51–4.35 (2H, m), 4.07–3.96 (2H, m), 3.69–3.55 (2H, m). The peak at 5.30 ppm refers to the CH_2Cl_2. Isolated yield: 95.2% (**Ni-1**), 94.3% (**Ni-2**).

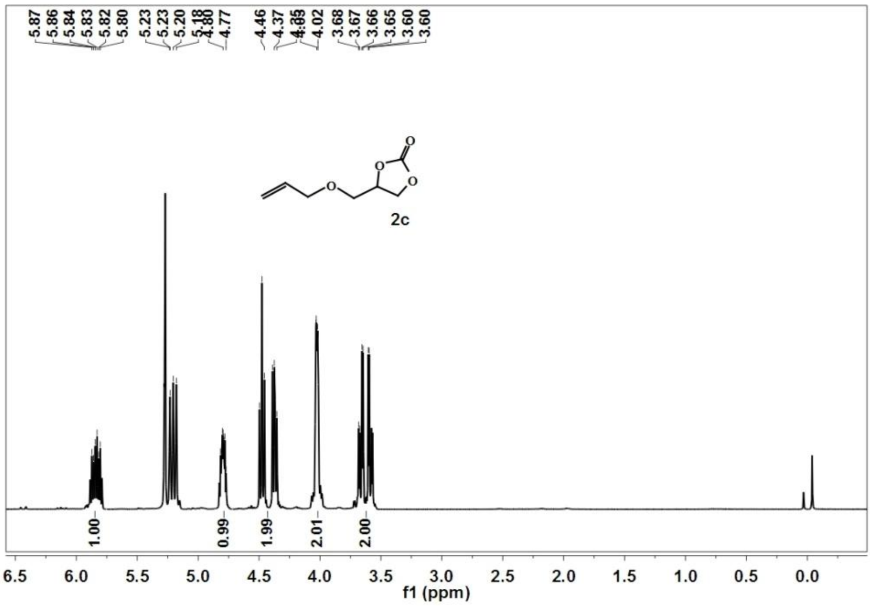

Figure S14. [1]H NMR spectra of 2d (400 MHz, $CDCl_3$): δ = 4.81 (1H, td, *J* 9.6, 3.8), 4.55–4.36 (2 H, m), 3.64 (2 H, ddd, *J* 27.3, 11.0, 3.8), 3.51 (2H, t, *J* 6.5), 1.59–1.53 (2H, m), 1.36 (2 H, dd, *J* 14.9, 7.4), 0.92 (3H, t, *J* 7.4). Isolated yield: 86.3% (**Ni-1**), 88.5% (**Ni-2**).

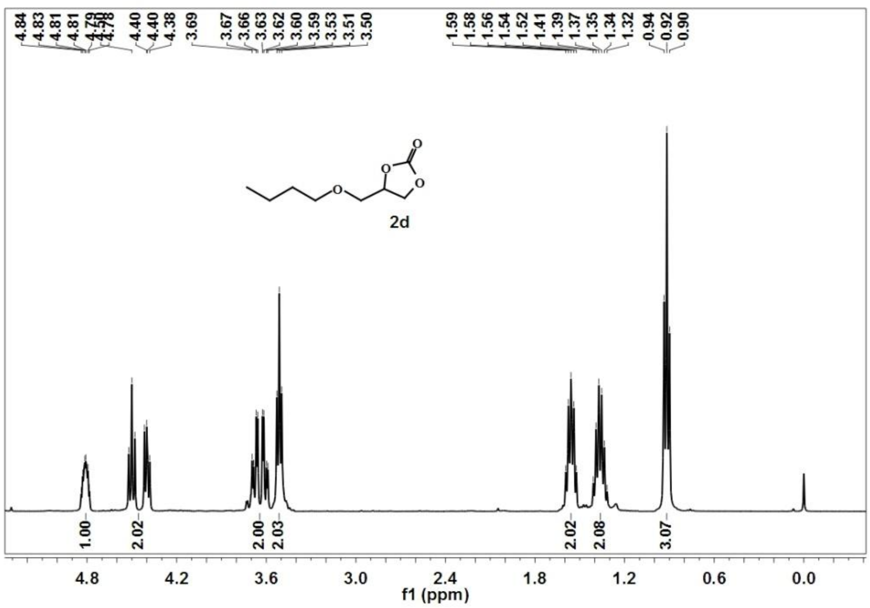

Figure S15. [1]H NMR spectra of 2e (400 MHz, $CDCl_3$): δ = 7.36–7.24 (2H, m), 7.11–6.75 (3H, m), 5.02 (1H, ddd, *J* 8.4, 4.2, 1.9), 4.65–4.48 (2H, m), 4.18 (2H, ddd, *J* 36.0, 10.5, 3.9). The peak at 5.30 ppm refers to the CH_2Cl_2. Isolated yield: 81.6% (**Ni-1**), 82.4% (**Ni-2**).